Is sea-ice-driven Eurasian cooling too weak in models?

James A. Screen & R. Blackport

ARISING FROM M. Mori et al. *Nature Climate Change* https://doi.org/10.1038/s41558-018-0379-3 (2019)

In a recent Letter, Mori et al.[1] examined connections in observations and climate models between reduced Arctic sea ice and the 'warm Arctic and cold Eurasia' (WACE) pattern. They concluded that models systemically underestimate Eurasian cooling in response to sea-ice loss, relative to observations. If correct, their result implies that up to half of the observed Eurasian cooling from 1995-2014 is attributable to sea-ice loss[1], whereas previous studies have found a negligible contribution from sea-ice loss[2-4]. Here, we highlight that their comparisons between observations and models are not like-for-like and when fair comparisons are made, modelled and observed estimates are consistent with each other. The upward adjustment of the contribution of sea-ice loss to observed Eurasian cooling in Mori et al.[1] is therefore unjustified.

An essential first step in model evaluation is to derive an observational benchmark against which models can be assessed. Mori et al. [1] seek an observational estimate of the WACE response to Barents-Kara sea-ice loss. Their approach is to correlate time-series of the WACE and Barents-Kara sea ice. They interpret the squared correlation coefficient multiplied by the WACE variance (hereafter $r^2\sigma^2$) as the fraction of WACE variance *driven* by sea ice. In doing so, they make an assumption about causality. Their apparent justification for this causal inference is that their analysis detects the WACE as the main pattern of sea-ice-driven temperature variability. However, the WACE also varies irrespective of sea ice and as a result, their observed time-series of the WACE (EC_{ERA}) contains variability driven by sea ice and variability not driven by sea ice. Importantly, even the non-sea-ice-driven component will correlate with Barents-Kara sea ice because a warm Arctic causes reduced sea ice, and vice versa. Sea ice and WACE variability will correlate because Arctic temperature and sea ice are strongly and physically connected, even if Eurasian temperature is minimally affected by sea ice, as recent work suggests[5]. For the reasons just given, the interpretation of $r^2\sigma^2$ as the fraction of WACE variance *driven* by sea ice is questionable and, as we will demonstrate, it is likely an overestimation.

Mori et al.[1] also calculate $r^2\sigma^2$ from atmospheric general circulation model (AGCM) experiments in which sea ice is specified. Interaction between ice and atmosphere is one-way in this experimental setup: the atmospheric response to varying sea ice is represented but the response of sea ice to atmospheric variation is not. Mori et al.[1] report that the observed $r^2\sigma^2$ is roughly twice as high as those obtained from seven different AGCMs, leading them to conclude that models systemically underestimate the WACE response to sea-ice loss. However, their comparison between observations and AGCMs is misleading because the observed $r^2\sigma^2$ reflects two-way interaction between sea ice and atmosphere whereas AGCM-derived $r^2\sigma^2$ only reflects the one-way influence of sea ice on the atmosphere.

Here, we test how much $r^2\sigma^2$ is suppressed by a lack of two-way interaction in AGCM simulations. We first reproduced the results of Mori et al.[1] (with minor methodological differences; see Methods), which confirms that none of the seven AGCMs reproduce the observed $r^2\sigma^2$ (Fig. 1a). It is important to note that this discrepancy is seen in both the winter months collectively (Fig. 1a) and in winter averages (c.f. Fig. 4a in Mori et al.[1]), which strongly suggests that the origin of the model-observation disparity is not time-scale dependent, and justifies our use of monthly averages in what follows. Next, we compared output from an atmosphere-ocean general circulation model (AOGCM) and an AGCM prescribed with sea ice and sea surface temperatures taken from the parent AOGCM (see Methods). The $r^2\sigma^2$ in the AOGCM experiment is roughly twice as high as in the AGCM (Fig. 1b), which we attribute to the simulation of two-way atmosphere-ice interaction in the AOGCM but not in the AGCM. The smaller $r^2\sigma^2$ in AGCMs compared to observations shown originally by Mori et al.[1] and reproduced here in Fig. 1a need not imply model error. Instead, it could be largely explained by the lack of two-way interaction in AGCM experiments and the inability of the $r^2\sigma^2$ method to extract the sea-ice-driven fraction of observed WACE variability. We caution not to directly compare the observed (Fig. 1a) and AOGCM-derived (Fig. 1b) $r^2\sigma^2$ as they correspond to different climate states. Although the observed $r^2\sigma^2$ is higher than in the AOGCM, this likely reflects greater sea-ice variability (by ~50%; not shown) in the recent past compared to the preindustrial climate, rather than model error.

We note that the higher $r^2\sigma^2$ in the AOGCM compared to the AGCM (Fig. 1b) could arise due to one of two reasons: because coupling is necessary to simulate the effects of WACE variability on sea ice or because ocean feedbacks could amplify the WACE response to sea-ice loss. Regarding the former, coupled models simulate the effects of WACE-related atmospheric circulation variability on Barents-Kara sea ice similarly to the real world[5]. Regarding the latter, it is clear that ocean feedbacks would strengthen the local warming response to sea-ice loss. However, this need not imply any change in Eurasian cooling. Indeed, Deser et al.[6] showed that ocean coupling enhanced the Arctic warming and atmospheric circulation responses to sea-ice loss, but suppressed Eurasian cooling. Surveying the literature, there is no evidence that coupled models simulate stronger Eurasian cooling in response to sea-ice loss than uncoupled models[6-10].

To gain further insight, and building upon Blackport et al.[5], we propose a refined approach to estimate the WACE variance driven by sea ice, which can be applied equally to observations and AGCMs. We hypothesise that a better estimate can be obtained from the correlation between the WACE and Barents-Kara sea ice in the preceding month, rather than using the contemporaneous correlation. Lead-lag correlation is a common first step in causal discovery and is physically justified here because the upward surface heat flux anomalies that might cause or reinforce the WACE tend to lag reductions in Barents-Kara sea ice[5,11]. Conversely, WACE-induced (and more generally, circulation-induced) downward heat flux anomalies tend to precede reductions in Barents-Kara sea ice[5,11]. Blackport et al.[5] presented evidence that this 1-month lead or 1-month lag approach can effectively distinguish between regimes of 'ice driving atmosphere' and 'atmosphere driving ice'. To test our hypothesis, we repeated the analysis but calculating $r^2\sigma^2$ with Barents-Kara sea ice one month ahead of the WACE (see Methods). The AOGCM and AGCM gave almost identical estimates of the WACE variance driven by sea ice when using the refined method (Fig. 1d), lending support to our hypothesis and suggesting that ocean coupling has little effect on the WACE response to sea-ice loss.

Applying the refined approach to the observations and AGCMs (Fig. 1c) leads to a rather different conclusion on model performance to that in Mori et al.[1]. Now, the estimates from all seven AGCMs lie close to that from observations. Only two AGCMs have ensemble member ranges that do not span the observed estimate, and only by very small margins (likely within observational uncertainty, which has not been accounted for here). We conclude that the modelled and observed estimates of the WACE variance driven by sea ice are consistent with each other. This suggests that AGCMs are able to realistically simulate the WACE response to sea-ice loss, effectively ruling out either AGCM error or lack of ocean coupling as the main reason for the stronger Eurasian cooling trends in observations compared to AGCMs.

Lastly, we repeated the analysis but calculating $r^2\sigma^2$ with Barents-Kara sea ice lagging one month behind the WACE. Now, $r^2\sigma^2$ provides an estimate of the WACE variance related to atmospheric driving of sea ice. $r^2\sigma^2$ is non-zero in the AGCMs partly because the imprint of observed WACE variability is contained in the sea ice conditions specified in the AGCMs. Also, due to serial correlation, the $r^2\sigma^2$ at 1-month lead (Fig. 1d,e) and 1-month lag (Fig. 1c,d) do not, and should not be expected to, sum to the contemporaneous $r^2\sigma^2$ (Fig. 1a,b). Nevertheless, when sea ice lags the WACE, we find a clear discrepancy between observations and AGCMs (Fig. 1e) and between the AOGCM and AGCM (Fig. 1f), in stark contrast to the consistency found when sea ice leads the WACE (Fig. 1c,d). This provides further evidence that the apparent divergence between observations and models reported by Mori et al.[1] stems from the inability of AGCM experiments to simulate the effects of the WACE on sea ice, and the failure of the original $r^2\sigma^2$ method to extract the sea-ice-driven fraction of observed WACE variability. This reasoning is likely valid across timescales, at least qualitatively, given that WACE-related weather patterns drive warming in the Arctic, thereby reducing sea ice, on sub-monthly[5,11-13], monthly[5,14,15], seasonal[5,16] and multidecadal[2-5,7,17] timescales.

In summary, here we have shown that the two main conclusions of Mori et al.[1] - that models systematically underestimate Eurasian cooling in response to Arctic sea-ice loss and that ~44% of observed Eurasian cooling is attributable to sea-ice loss - were based upon a misleading comparison of observations and models. When fair comparisons are made, observations and models agree on the fraction of WACE variance driven by sea ice. There is therefore, no justification for the adjustment to the model output that leads Mori et al.[1] to conclude that 32-51% of observed Eurasian winter cooling from 1995-2014 is attributable to sea-ice loss. Without this misleading adjustment, models suggest that sea-ice loss has contributed little to colder Eurasian winters, which can instead be largely explained as a manifestation of internal climate varaibility[2-5].

References

1. Mori, M., Kosaka, Y., Watanabe, M., Nakamura, H. & Kimoto, M. A reconciled estimate of the influence of Arctic sea-ice loss on recent Eurasian cooling. *Nat. Clim. Change* **9**, 123–129 (2019).
2. McCusker, K. E., Fyfe, J. C. & Sigmond, M. Twenty-five winters of unexpected Eurasian cooling unlikely due to Arctic sea-ice loss. *Nat. Geosci.* **9**, 838–842 (2016).
3. Sun, L., Perlwitz, J. & Hoerling, M. What caused the recent "Warm Arctic, Cold Continents" trend pattern in winter temperatures? *Geophys. Res. Lett.* **43**, 5345–5352 (2016).
4. Ogawa, F. et al. Evaluating impacts of recent Arctic sea ice loss on the northern hemisphere winter climate change. *Geophys. Res. Lett.* **45**, 3255–3263 (2018).
5. Blackport, R., Screen, J., van der Wiel, K. & Bintanja, R. Minimal influence of reduced Arctic sea ice on coincident cold winters in mid-latitudes. *Nat. Clim. Change* **9**, 697-704 (2019).
6. Deser, C., Sun, L., Tomas, R. A. & Screen, J. Does ocean coupling matter for the northern extratropical response to projected Arctic sea ice loss? *Geophys. Res. Lett.* **43**, 2149-2157 (2016).

7. Smith, D., Dunstone, N., Scaife, A., Fiedler, E., Copsey, D. & Hardiman, S. Atmospheric response to Arctic and Antarctic sea ice: The importance of ocean-atmosphere coupling and the background state. *J. Clim.* **30**, 4547-4565 (2017).
8. Collow, T., Wang, W. & Kumar, A. Simulations of Eurasian winter temperature trends in coupled and uncoupled CFSv2. *Adv. Atmos. Sci.* **35**, 14-26 (2018).
9. Sun, L., Alexander, M. & Deser, C. Evolution of the global coupled climate response to Arctic sea ice loss during 1990-2090 and its contribution to climate change. *J. Clim.* **31**, 7823-7843 (2018).
10. Screen, J., et al. Consistency and discrepancy in the atmospheric response to Arctic sea-ice loss across climate models. *Nat. Geosci.* **11**, 153-163 (2018).
11. Sorokina, S. A., Li, C., Wettstein, J. J. & Kvamstø, N. G. Observed atmospheric coupling between Barents Sea ice and the warm-Arctic cold-Siberian anomaly pattern. *J. Clim.* **29**, 495–511 (2016).
12. McGraw, M. & Barnes, E. New insights on subseasonal Arctic-midlatitude causal connections from a regularized regression model. *J. Clim.* doi:10.1175/JCLI-D-19-0142.1 (2019).
13. Gong, T. & Luo, D. Ural blocking as an amplifier of the Arctic sea ice decline in winter. *J. Clim*. **30**, 2639-2654 (2017).
14. Sato, K., Inoue, J. & Watanabe, M. Influence of the Gulf Stream on the Barents Sea ice retreat and Eurasian coldness during early winter. *Environ. Res. Lett.* **9**, 084009 (2014).
15. Peings, Y. Ural blocking as a driver of early-winter stratospheric warmings. *Geophys. Res. Lett.* **46**, 5460-5468 (2019).
16. Kelleher, M. & Screen, J. Atmospheric precursors of and response to anomalous Arctic sea ice in CMIP5 models. *Adv. Atmos. Sci.* **35**, 27-37 (2018).
17. Sung, M., Kim, S., Kim, B. & Choi, Y. Interdecadal variability of the warm Arctic and cold Eurasia patterns and its North Atlantic origin. *J. Clim.* **31**, 5793-5810 (2018).
18. Kay, J. E., et al. The Community Earth System Model (CESM) large ensemble project: A community resource for studying climate change in the presence of internal climate variability. *Bull. Amer. Meteor. Soc.* **96**, 1333-1349 (2015).
19. Chen, H. & Schneider, E. K. Comparison of the SST-forced responses between coupled and uncoupled climate simulations. *J. Clim*. **27**, 740–756 (2014).
20. Zhou, Z., Xie, S., Zhang, G. J. & Zhou, W. Evaluating AMIP skill in simulating interannual variability over the Indo–Western Pacific. *J. Clim.* **31**, 2253–2265, (2018).

Methods

In Fig. 1a,c,e, we use the exact same data as Mori et al.[1]. Briefly, observational results come from the ERA-Interim reanalysis for the period 1979-2014 and modelled results come from seven AGCM simulations in which observed sea surface temperatures and sea ice have been specified. Further details on these model simulations can be found in Mori et al.[1]. Additionally in Fig. 1b,d,f, we analyse two experiments performed as part of the Community Earth System Model (CESM) Large Ensemble project[18]. The first is a 200-year section (years 401-600) of a preindustrial control run of the CESM configured with the Community Atmosphere Model version 5 (CAM5). CESM-CAM5 is a global coupled climate model at approximately 1° horizontal resolution in all model components. The second additional experiment is a 200-year simulation with CAM5 in which sea surface temperatures and sea ice were specified from years 401-600 of the parent CESM-CAM5 simulation. External forcing is the same in both simulations. Initially in Fig. 1a, we employed the same methodologies as Mori et al.[1] to calculate the WACE pattern, the WACE time-series and the Barents-Kara sea-ice index (see Mori et al.[1] for details), with one exception. We computed the WACE and Barents-Kara sea-ice time-series from monthly averages whereas Mori et al.[1] used winter averages. The purpose of this modification is to facilitate subseasonal lead-lag correlations. Projecting near-surface temperatures for December, January and February separately onto the winter-mean WACE pattern produced monthly WACE time-series. Fig. 1a shows the total and sea-ice-driven variance for the three winter months combined. To construct Fig. 1b, we performed an analogous analysis but substituted data from ERA-Interim with that from CESM-CAM5. More specifically, we derived the WACE pattern as the leading mode of covariability from singular value decomposition applied to the CESM-CAM5 and CAM5 simulations. The r^2 was then calculated by correlating the corresponding WACE time-series with the Barents-Kara sea-ice index from CESM-CAM5. In this so-called "perfect model" comparison[19,20], the coupled model simulation is an analogue for the observations and therefore, any difference between the CESM-CAM5 and CAM5 results can be attributed solely to ocean coupling. To construct Fig. 1c-f, we adapted the Mori et al.[1] approach by introducing a 1-month lead or lag time between the WACE and Barents-Kara sea-ice time-series. In Fig1c,d we show the combination of three cases where the Barents-Kara sea-ice index leads the WACE time-series by one month: November sea ice correlated with December WACE, December sea ice correlated with January WACE, and January sea ice correlated with February WACE. In Fig1c,d we show the combination of three cases where the Barents-Kara sea-ice index lags the WACE time-series by one month: January sea ice correlated with December WACE, February sea ice correlated with January WACE, and March sea ice correlated with February WACE.

Acknowledgements. The authors thank Masato Mori for providing data from the MIROC simulations and for useful discussions. We acknowledge the individuals and modelling groups that contributed to the Facility for Climate Assessments (FACTS) multimodel data set and the CESM Large Ensemble Project.

Data availability. The FACTS and CESM simulations are freely available and were obtained from the following repositories: https://www.esrl.noaa.gov/psd/repository/facts and https://www.cesm.ucar.edu/projects/community-projects/LENS/.

Contributions. J.A.S and R.B. jointly conceived the analysis. R.B. created Fig. 1. J.A.S. wrote the manuscript with input from R.B.

Competing interests. The authors declare no competing interests.

Corresponding author. Correspondence to J. A. Screen

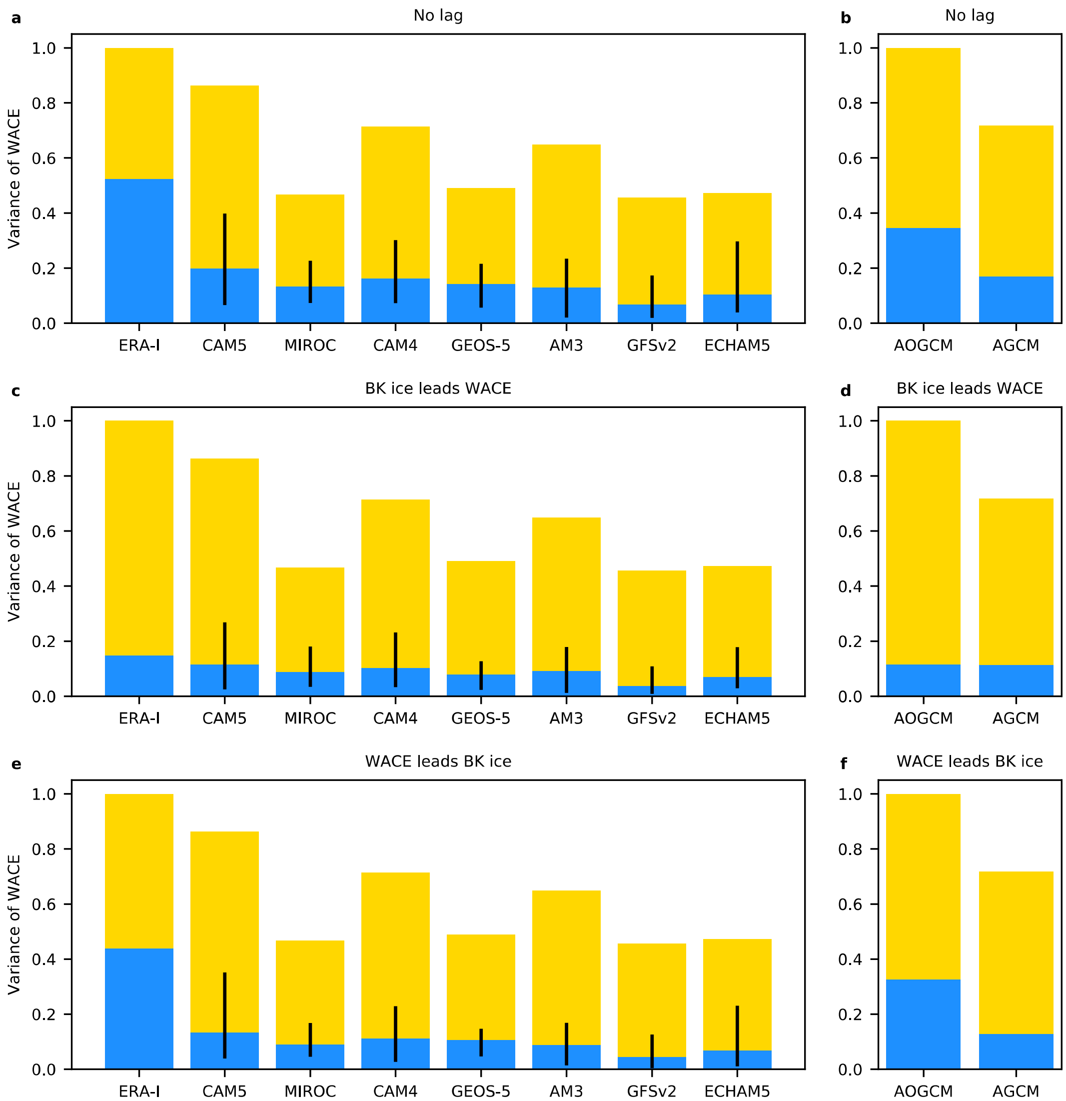

Figure 1. Observed and modelled estimates of the total and sea-ice-driven WACE variance. a, Total variance of WACE for ERA-Interim and seven AGCM experiments (blue plus yellow bars). The vertical axis in **a** is scaled by the total WACE variance in ERA-Interim. The blue bars show the variance explained by Barents-Kara sea ice estimated from $r^2\sigma^2$. For the AGCMs, the bars show results for all ensemble members (concatenated in series) and the vertical black lines provide the ensemble ranges. **b**, As (**a**) but for a single AGCM (CAM5) and it's parent AOGCM (CESM-CAM5). The vertical axis in **b** is scaled by the total WACE variance in the coupled model. **c**,**d**, As (**a**,**b**) but calculating $r^2\sigma^2$ with Barents-Kara sea ice one month ahead of the WACE. **e**,**f**, As (**a**,**b**) but calculating $r^2\sigma^2$ with Barents-Kara sea ice one month behind the WACE.